A Study on Multipath Spatial Correlation for GNSS Collaborative Positioning

Guohao Zhang[1], Lucy Icking[2], Li-Ta Hsu[1] and Steffen Schön[2]
[1]*Department of Aeronautical and Aviation Engineering, The Hong Kong Polytechnic University, Hong Kong, China;*
[2]*Institut für Erdmessung, Leibniz Universität Hannover, Hannover, Germany;*

ABSTRACT

The accuracy of GNSS positioning is significantly degraded in urban areas, due to the signal reflections from buildings. The 3D mapping aided (3DMA) GNSS based collaborative positioning, integrating the 3DMA GNSS ray-tracing algorithm with the GNSS collaborative positioning, can sufficiently improve the positioning accuracy in the urban area, by eliminating the systematic errors and mitigating the multipath and NLOS reception errors simultaneously. However, the effectiveness of the collaborating agent or the collaborator selection strategy for a target agent in the urban area has not been investigated yet. The collaborating agent selection strategy based on the environment context or the measurement spatial correlation will be analyzed. Simulation result shows, collaborating with the agents from the open-sky environment can ensure the qualities of anchor positions and achieve a better collaborative positioning performance. On the other hand, the measurement spatial correlation occurs for the agents with similar environment geometry and improves the quality of relative position constraints during the collaborative positioning. As a result, collaborating with the spatial correlated agents can also achieve an accurate collaborative positioning solution comparing to the collaboration with open-sky agents.

1. INTRODUCTION

An accurate positioning solution is essential to guarantee the quality of personal navigation or location-based services (LBS). Among various sensors conducting localization, the global satellite navigation system (GNSS) plays a key role, which directly provides the absolute positioning solution and maintains economical to the mass market. However, the GNSS signal can be easily interfered during its propagation, introducing a certain delay in the ranging measurement, such as the tropospheric and ionospheric delay. Instead of applying model-based corrections, due to the recent development of communication technology, new approaches have been proposed to collaborate with the neighboring road agents to eliminate those systematic errors shared in a certain region [1-3], namely the collaborative positioning (CP). In fact, the collaboration with multiple agents can obtain additional benefits, for example, the reduction of measurement noise [4], additional information in a restricted environment [5], and the ability of anti-spoofing [6].

However, the performance of GNSS-based collaborative positioning can be significantly degraded by outliers that are unique to a specific user. The multipath or non-line-of-sight (NLOS) delays in the urban area are highly related to the signal propagation geometry [7]. Those interferences can introduce over 50 meters of positioning errors, and are unable to be directly mitigated by collaborating with other users. It is necessary to apply multipath/NLOS mitigation techniques in the meantime of collaborative positioning. A straightforward method is to employ the measurement carrier-to-noise ratio (C/N_0) to distinguish and de-weight the measurements degraded by multipath or NLOS reception [8, 9]. Unfortunately, the C/N_0 of a reflection interfered signal can be similar to a line-of-sight (LOS) signal, which makes the weighting improper. Another popular method to mitigate those interferences is to adapt the receiver autonomous integrity monitoring (RAIM) technique and to apply a consistency check for the measurements [10, 11]. However, for urban areas with many interferences, the consistency check may fail to distinguish healthy measurements from multiple outliers. Even worse, only a few satellites are available and shared by the users during collaborative positioning, limiting the performance of consistency checks [12].

A potential approach to maintain the collaborative positioning performance in complicated urban areas is integrating the 3D mapping aided (3DMA) GNSS algorithm, which not only mitigates but also makes use of the multipath and NLOS reception. One of the popular 3DMA GNSS techniques, Shadow Matching [13], localizes the user by examining the similarity of the satellite visibility between the measurement estimation and the building-model-based prediction. By complementarily integrating Shadow Matching with collaborative positioning [14], both the cross- and along-street positioning can be improved by employing visibility matching and visibility-based NLOS exclusion, respectively. Shadow Matching can also be extended by the inter-agent ranging measurement from other sensors in the collaborative positioning manner to reduce the positioning uncertainty [15]. Another 3DMA GNSS technique, ray-tracing [16], localizes the user by the pseudorange similarity between the received measurement and the building-model-based prediction, including the NLOS delay. By integrating ray-tracing with collaborative

 https://doi.org/10.33012/2021.17942

positioning [17], the measurement degradation can be used as additional information to guarantee the collaborative positioning performance even in a dense urban area.

Besides the benefits of positioning accuracy, other issues related to the practical applications of collaborative positioning need to be investigated. The scalability of the 3DMA GNSS based collaborative positioning algorithm [17] in terms of accuracy and computation load has been studied in [18]. The analysis result shows that, for an open-sky scenario, the collaborative positioning accuracy and robustness will be improved by a large collaboration network, but the advantage is gradually reduced after the network exceeds a certain size. However, for an urban environment, the positioning accuracy may start being reduced after a certain network size, due to the involvement of more severely degraded collaborators. Meanwhile, the computational load from a larger network is increased in a squared manner, which severely restricts practical applications. Therefore, it is necessary to apply a collaborator selection before conducting the collaborative positioning to guarantee performance and effectiveness.

A straightforward strategy is to select agents in an open-sky environment with less degraded GNSS measurements to collaborate with the target agent located in the urban area. Those open-sky agents with better positioning accuracy can be used as accurate anchors during the collaboration. However, although the systematic errors can be effectively eliminated, the unique delay from multipath or NLOS reception remains. Even by employing 3DMA GNSS ray-tracing, those unique errors cannot be perfectly corrected, and its residuals still degrade the accuracy. Consequently, the performance improvement could be limited when only collaborating with agents from the open-sky environment.

According to the study in [19], the multipath or NLOS delay is closely related to the surrounding environment and the geometrical parameters during the signal propagation. In other words, the agents in a similar urban environment may experience a spatially correlated multipath/NLOS delay. Fig. 1 shows the delay behavior of the reflected signal from buildings on different locations across a street. The distance of an agent towards the building affects both the availability and the delay of the reflected signal. Hence, agents with the same distance to the reflecting surfaces are expected to show similar reflection delays, meaning that a high correlation of errors is provided when agents are located in a line parallel to the facades. By selecting those agents for collaborative positioning, the multipath/NLOS delay becomes a shared error that can be mitigated via collaboration.

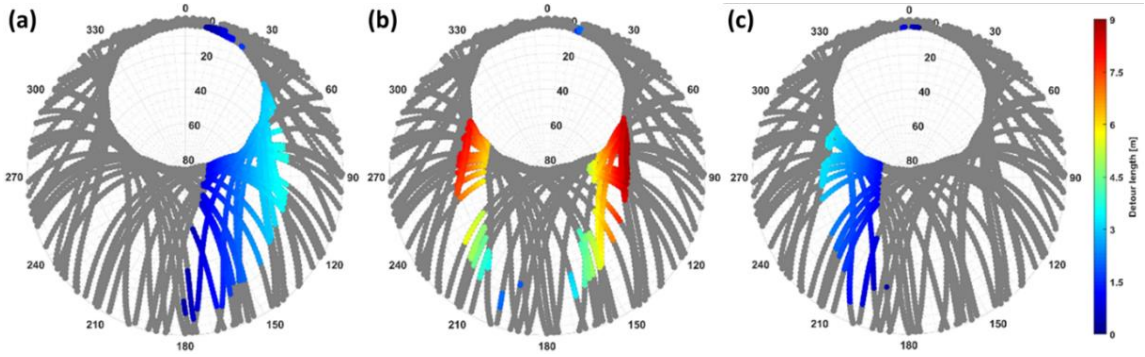

Fig. 1 Simulation of the variation of extra path lengths of GPS satellites across a street in skyplots. (a) Agent on the west side of a street oriented in north/south direction, (b) in the middle, (c) on the east side of the street. The street width is around 12 meters, and the building heights are around 20 meters.

In this study, a collaborator selection strategy based on the operating environment will be firstly studied for collaborative positioning. By employing a realistic urban GNSS simulator [20], the measurements of agents with interferences in different environments will be simulated. The positioning performance of a target agent under the collaboration with open-sky agents will be evaluated and compared to the collaboration without any selection via the Monte Carlo method. Then, the measurements of multiple agents lined up on the along-/cross-direction of a street are simulated to investigate the spatial correlation on the pseudorange. After that, the benefits of spatial correlation on relative positioning during collaboration will be analyzed. Finally, the performance of collaborative positioning with spatially correlated agents will be evaluated and compared with the collaboration of open-sky agents. The contributions of this study are twofold: 1) the investigation on an effective collaborator selection strategy based on the surrounding environment for practical collaborative positioning algorithms; 2) the analysis of multipath/NLOS correlation in the urban environment and its benefits on aiding the collaborative positioning performance.

The remainder of this paper is structured as follows. A brief introduction to the 3DMA GNSS based collaborative positioning algorithm used for investigation is given in Section 2. The simulation platform employed for analysis will be briefly introduced in Section 3. In Section 4, the collaborator selection strategy based on environment context will be analyzed by a large-scale simulation. Then, the analysis of measurement spatial correlation and its benefits on the positioning is given in Section 5. Finally, the conclusion is drawn with suggested future works in Section 6.

2. BRIEF INTRODUCTION TO 3DMA GNSS COLLABORATIVE POSITIONING ALGORITHM

2.1. System Architecture

In this study, the analysis on the collaboration with different agents is conducted based on the 3DMA GNSS collaborative positioning algorithm developed in [17], which is applicable even in a dense urban environment. The system architecture is shown in Fig. 2. The GNSS raw measurement of each agent will be firstly applied with the 3DMA GNSS ray-tracing positioning [16] to obtain the absolute position constraint, based on the database of pre-simulated GNSS LOS/NLOS ranges on different candidate locations (grids) nearby the agent [21]. Here, the resolution of grids is 2-by-2 meters. Meanwhile, grids having similar pseudoranges to the received measurements are regarded as effective grids, which will be paired with those from another agent for relative positioning. The relative position constraint between different agents is determined by comparing the consistency of the inter-position from grid locations and double-difference (DD) estimation with NLOS correction, namely the grid-based 3DMA GNSS relative positioning. The details will be explained in Section 2.2. Besides, based on the velocity estimation from Doppler shift measurement, the inter-epoch dynamic constraint can be estimated for each agent [17]. Finally, the absolute position constraints, relative position constraints, and inter-epoch dynamic constraints of all the involving agents construct a factor graph connecting all historical data for optimization [22], obtaining the improved position solution for different agents.

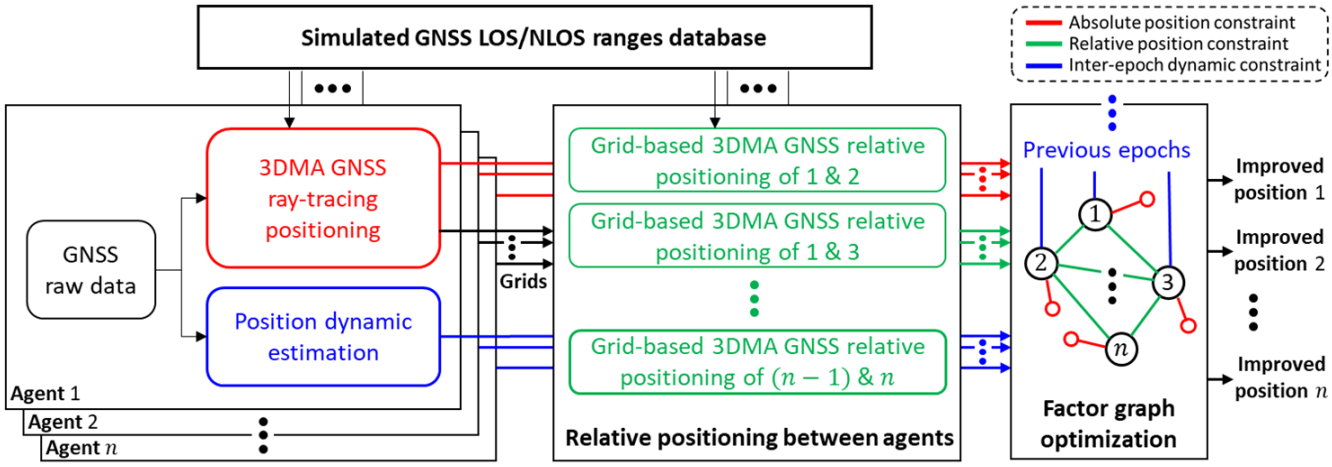

Fig. 2 The system architecture of the 3DMA GNSS based collaborative positioning algorithm.

2.2. Grid-based 3DMA GNSS Relative Positioning with Ray-tracing and DD

The relative position constraint of the employed collaborative positioning algorithm is obtained by integrating the double difference positioning with the 3DMA GNSS ray-tracing algorithm, to mitigate the NLOS reception error [17]. The pseudorange measurement from the i^{th} satellite to the n^{th} agent can be described by

$$\rho_n^i = r_n^i + \delta\rho_{rcvr,n} + \delta\rho_{sv}^i + \epsilon_n^i \tag{1}$$

where $\delta\rho_{rcvr,n}$ is the receiver clock offset, $\delta\rho_{sv}^i$ is the satellite-related error term including the ionospheric delay, tropospheric delay, and satellite clock or orbit bias. ϵ_n^i denotes the pseudorange error term that is unique to each satellite and each agent, such as the multipath or NLOS error. Based on the measurements from agents *a* and *b* as well as the master satellite *m* (usually selects the satellite with the highest elevation angle), the DD measurement can be derived by

$$d_{ab}^{im} = \left(\rho_b^m - \rho_b^i\right) - \left(\rho_a^m - \rho_a^i\right) \tag{2}$$

Although the DD measurement eliminates the $\delta\rho_{rcvr,n}$ and $\delta\rho_{sv}^i$ error terms, the unique error terms related to ϵ_a^i, ϵ_b^i, ϵ_a^m, and ϵ_b^m still remain and require mitigation before the relative positioning. Suppose agent a and b have k_a and k_b effective grids during the 3DMA GNSS ray-tracing positioning (red block in Fig. 2), the NLOS delay simulated by ray-tracing on grid k_a and k_b can be employed to correct the degraded DD measurement, denoted as $d_{k_a k_b}^{im}$. For this pair of grids, the relationship between their relative position and the corresponding NLOS-mitigated DD measurement can be described by

$$d_{k_a k_b}^{im} = (\boldsymbol{\eta}^m - \boldsymbol{\eta}^i) \cdot \Delta\hat{\boldsymbol{x}}_{k_a k_b} \tag{3}$$

where $\boldsymbol{\eta}^i$ and $\boldsymbol{\eta}^m$ are the unit-LOS vectors of the i^{th} and m satellite, respectively. After collecting the corrected DD measurement from 1 to i^{th} satellite, the corresponding relative position $\Delta\widehat{\boldsymbol{x}}_{k_a k_b}$ for this pair of grids can be estimated via pseudo-inverse and least-squares estimation. This pseudo-inverse requires at least 4 shared satellites between this pair of grids, including the master satellite. By checking the consistency between this estimated relative position $\Delta\widehat{\boldsymbol{x}}_{k_a k_b}$ and the actual relative grid position $\Delta\widetilde{\boldsymbol{x}}_{k_a k_b}$ between the selected grid k_a and k_b, the correctness of the corresponding ray-tracing can be evaluated. Then, among the total of $K_{ab} = k_a \cdot k_b$ pairs of grids between agent *a* and *b*, the top 1% pairs (denoted by K_{ab}^*) with better consistency of $\Delta\widehat{\boldsymbol{x}}_{k_a k_b}$ and $\Delta\widetilde{\boldsymbol{x}}_{k_a k_b}$ are selected to estimate the relative position constraint between agent *a* and *b*, using

$$\Delta\widehat{\boldsymbol{x}}_{ab} = \left(\sum_{K_{ab}^*} \Lambda_{K_{ab}^*} \cdot \Delta\widetilde{\boldsymbol{x}}_{K_{ab}^*}\right) / \sum_{K_{ab}^*} \Lambda_{K_{ab}^*} \tag{4}$$

Where $\Delta\widetilde{\boldsymbol{x}}_{K_{ab}^*}$ is the relative grid position of each selected pair of grids, and $\Lambda_{K_{ab}^*}$ is the weighting of each selected pair of grids obtained from the preceding consistency level [17], a higher consistency has a higher weighting.

2.3. Factor Graph Optimization

After collecting all the absolute position constraints from the 3DMA GNSS ray-tracing positioning (red line in Fig. 2), relative position constraints from the grid-based 3DMA GNSS relative positioning (green line in Fig. 2), and the inter-epoch dynamic constraints from Doppler measurements (blue line in Fig. 2), those constraints are used to construct a factor graph to optimize the position of each agent in the collaboration. For agent *a*, the cost from absolute positioning constraint at epoch *t* is

$$\varepsilon_{a,t} = \boldsymbol{x}_{a,t} - \widehat{\boldsymbol{x}}_{a,t} \tag{5}$$

where $\boldsymbol{x}_{a,t}$ is the agent position that needs to be optimized, and $\widehat{\boldsymbol{x}}_{a,t}$ denotes the absolute constraint. The cost from relative positioning constraint between agent *a* and *b* at epoch *t* is

$$\varepsilon_{ab,t} = \boldsymbol{x}_{b,t} - \boldsymbol{x}_{a,t} - \Delta\widehat{\boldsymbol{x}}_{ab,t} \tag{6}$$

The cost from inter-epoch dynamic constraint for agent *a* between epoch t and $t-1$ is

$$\varepsilon_{a,t-1\to t} = \boldsymbol{x}_{a,t} - \boldsymbol{x}_{a,t-1} - \Delta\widehat{\boldsymbol{x}}_{a,t-1\to t} \tag{7}$$

where $\Delta\widehat{\boldsymbol{x}}_{a,t-1\to t}$ denotes the inter-epoch dynamic constraint. Then, for the collaborative positioning with *N* agents and *T* epochs, the overall objective function is

$$\boldsymbol{\chi}^* = \underset{\boldsymbol{\chi}}{arg\,min}\left(\sum_{t=1}^{T}\sum_{a=1}^{N}\left\|\varepsilon_{a,t}\right\|^2_{\boldsymbol{\Omega}_{a,t}^{-1}} + \sum_{t=1}^{T}\sum_{b=2}^{N}\sum_{a=1}^{N-1}\left\|\varepsilon_{ab,t}\right\|^2_{\boldsymbol{\Omega}_{ab,t}^{-1}} + \sum_{t=2}^{T}\sum_{a=1}^{N}\left\|\varepsilon_{a,t-1\to t}\right\|^2_{\boldsymbol{\Omega}_{a,t-1\to t}^{-1}}\right) \tag{8}$$

where $\boldsymbol{\chi} = \left[\boldsymbol{x}_{1,1}', \cdots, \boldsymbol{x}_{N,1}', \cdots, \boldsymbol{x}_{1,T}', \cdots, \boldsymbol{x}_{N,T}'\right]'$ is the vector combining the position vector of each agent on each epoch, and $\boldsymbol{\Omega}$ denotes the noise covariance matrix of the constraint. $\boldsymbol{\chi}^*$ denotes the final optimized position vector including all the collaborating agents.

3. SIMULATION PLATFORM

The analysis of the collaborative positioning performance in terms of the agent surrounding environments requires a large amount of GNSS data from receivers on different locations simultaneously. Since it is very difficult to be accomplished by real experiments, the analysis in this study is based on the simulated measurements from a realistic urban GNSS measurement simulator [20]. This simulator is capable of simulating GNSS raw measurements including interferences from signal reflection, diffraction or blockage due to buildings for multiple agents in urban areas. The overall flow chart is shown in Fig. 3.

Based on the location of each agent, the satellite position from the ephemeris and the building surface location described by the 3D building model, the simulator uses ray-tracing to search for valid LOS, reflection, and diffraction path of the GNSS signal. The measurement from each satellite will be classified into four types: LOS only, diffraction only, reflection only, and multipath. Then, the GNSS measurement will be simulated according to its type.

For the C/N_0 measurement, the LOS case is simulated based on a regression model developed from open-sky C/N_0 data. The C/N_0 of a diffraction only or reflection only case is simulated by combining the LOS C/N_0 with the uniform geometrical theory of diffraction (UTD) model [23] or the GNSS reflectometer (GNSS-R) model [24], respectively. The C/N_0 of the multipath case is simulated based on the superposition of the electro-magnetic fields of the top two effective signals. The GNSS ranging measurement is simulated based on the total propagation distance of the ray-tracing signal path for the LOS only, diffraction only, or reflection only case. For the multipath case, the corresponding ranging measurement is simulated based on the multipath noise envelope [25] with knowledge about the delay and C/N_0 of each involved signal. The Doppler shift measurement for the LOS only case is simulated based on the traditional Doppler shift model with knowledge about the signal property and the dynamics of the agent. For the cases of diffraction only, reflection only, and multipath, the Doppler shift measurement is simulated based on the Doppler shift model with a single intermediate point [26].

Finally, according to the receiver parameters and models, the simulated C/N_0, ranging, and Doppler shift measurements will be integrated with the systematic error or noise, including the tracking loop noise, atmospheric delays, receiver clock bias, etc. The resulting measurements of different agents are at the same level as the Receiver Independent Exchange Format (RINEX), which can be directly applied with the preceding 3DMA GNSS based collaborative positioning algorithm.

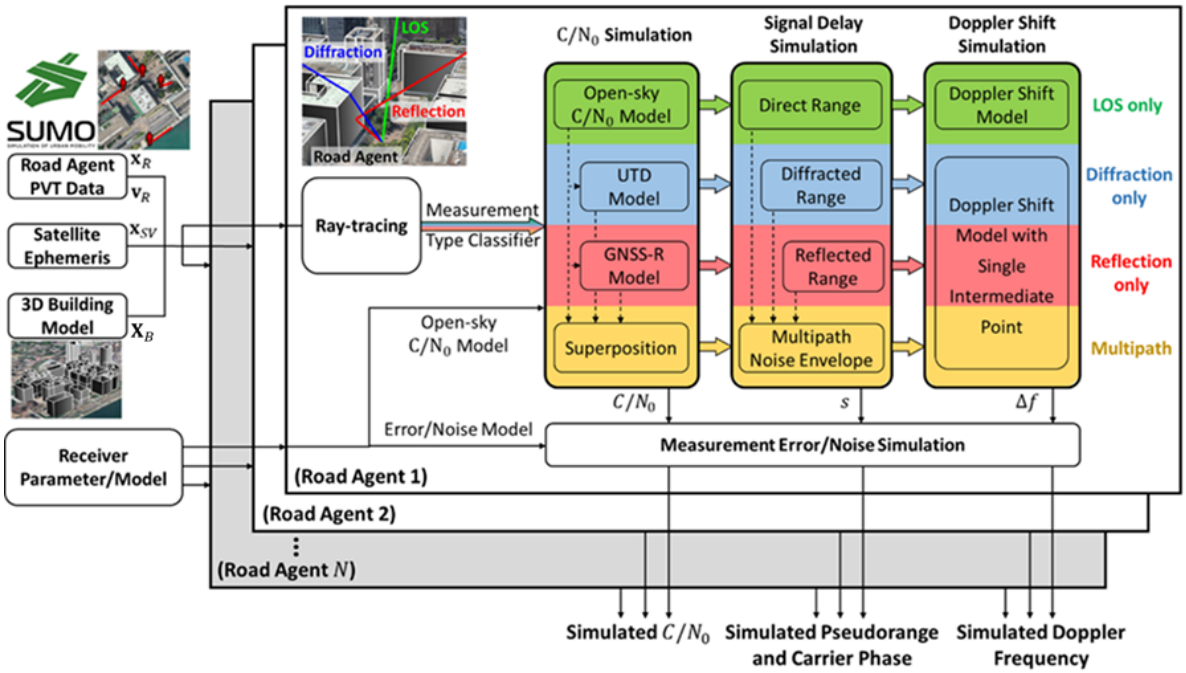

Fig. 3 Flow chart of the employed GNSS realistic urban multi-agent simulator (GNSS-RUMS) [20].

4. PERFORMANCE ANALYSIS ON AGENT SELECTION STRATEGY BASED ON ENVIRONMENT

Since a larger agent network may increase the computational load and involve more errors for the collaborative positioning, a collaborator selection strategy needs to be applied beforehand. A straightforward approach is to select collaborators based on the operating environment, which is closely related to the positioning error of each agent. In this section, we first set up a simulation with multiple agents in different environments. Then, the collaborative positioning performance with the agents from different environments (open-sky, urban area, or mixed) and the effectiveness of this environment-based collaborator selection strategy will be analyzed.

4.1. Simulation Setup

To conduct the analysis, the GNSS raw measurements of 50 static agents on different locations of an urban area are simulated based on the GNSS-RUMS. Here, 26 seconds of 1 Hz GNSS measurements from GPS and Beidou satellites are simulated for collaborative positioning. The location and averaged least-squares positioning error of each agent are demonstrated in Fig. 4. We use the averaged building elevation angle to quantify the urbanization level of the environment [27], defined as

$$\overline{el}_{BB} = \sum_{az=1}^{360} \theta_{BB,az}/360 \tag{9}$$

where $\theta_{BB,az}$ is the elevation angle of the building's upper boundary on the azimuth angle az. $\overline{el}_{BB}$ describes the severity of the sky being blocked by the buildings and associates to the GNSS positioning performance. As Fig. 4 (b) shows, the agent with a lower $\overline{el}_{BB}$ is located in an environment close to open-sky and obtains good GNSS performance, whereas the agent with a higher $\overline{el}_{BB}$ is located in a dense urban environment under severe GNSS degradation. In this simulation, the averaged building elevation angle of 50 agents range from around 5° to 73°, covering most of the environments for urban positioning. Among 50 agents, agents with $\overline{el}_{BB}$ below 15°, between 15° and 48°, and over 48° are categorized as open-sky, middle urban, and dense urban agents, respectively. The agent index is sorted by the averaged sky-view blockage ratio in an ascent manner before being assigned to different agents. The agent with a lower index number has a better sky-view.

After the simulation, we choose a target agent and apply the Monte Carlo method to randomly select its collaborator according to three different selection strategies:

(1) Open-sky CP: Select collaborator from open-sky agents ($\overline{el}_{BB}$ below 15°);
(2) Mixed CP: Select collaborator from all available agents;
(3) Dense urban CP: Select collaborator from dense urban agents ($\overline{el}_{BB}$ over 48°).

Since the network size also affects the collaborative positioning performance, the Monte Carlo method will be repeated on different network sizes for each selection strategy. Then, the collaborative positioning performances of the target agent using different collaborator selection strategies will be evaluated. In this study, the optimization during collaborative positioning is applied based on the true covariance of the absolute and relative position constraints, in order to evaluate the potential of the agent selection strategy and to avoid the influence from incorrect covariance estimation. The true covariance matrices for the absolute and relative position constraints, denoted as $\widetilde{\boldsymbol{\Omega}}_{a,t}$ and $\widetilde{\boldsymbol{\Omega}}_{ab,t}$, are obtained by

$$\widetilde{\boldsymbol{\Omega}}_{a,t} = \begin{bmatrix} \left(\tilde{x}_{a,t}^{East} - \hat{x}_{a,t}^{East}\right)^2 & 0 \\ 0 & \left(\tilde{x}_{a,t}^{North} - \hat{x}_{a,t}^{North}\right)^2 \end{bmatrix} \tag{10}$$

$$\widetilde{\boldsymbol{\Omega}}_{ab,t} = \begin{bmatrix} \left(\tilde{x}_{b,t}^{East} - \tilde{x}_{a,t}^{East} - \hat{x}_{ab,t}^{East}\right)^2 & 0 \\ 0 & \left(\tilde{x}_{b,t}^{North} - \tilde{x}_{a,t}^{North} - \hat{x}_{ab,t}^{North}\right)^2 \end{bmatrix} \tag{11}$$

where $\tilde{x}_{a,t}^{East}$ and $\tilde{x}_{a,t}^{North}$ are the true positions of agent a in East and North direction, $\hat{x}_{a,t}^{East}$ and $\hat{x}_{a,t}^{North}$ are the absolute positioning constraints $\hat{\boldsymbol{x}}_{a,t}$ resolved in East and North direction, $\hat{x}_{ab,t}^{East}$ and $\hat{x}_{ab,t}^{North}$ are the relative positioning constraints $\hat{\boldsymbol{x}}_{ab,t}$ resolved in East and North direction. Finally, by selecting different agents as the target agent and applying the same evaluation, the influence of the agent selection strategy will be analyzed.

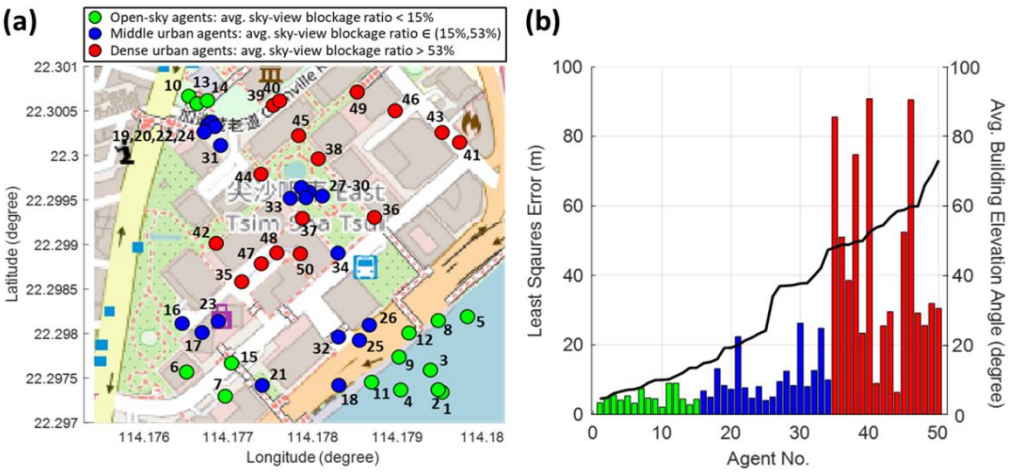

Fig. 4 (a) Location of each agent for GNSS measurement simulation during the agent selection strategy analysis; (b) Averaged least-squares error of the simulated measurement for each agent (colored bars), and the corresponding averaged building elevation angle (black line) denoting the environment context. The agent index sequence is corresponding to the averaged building elevation angle.

4.2. Collaborative Positioning Performance from Different Agent Selection Strategy

We firstly select agent 33 located in a middle urban environment as the target agent to evaluate the collaborative positioning performance from different agent selection strategies. The ground truth location and the GNSS least-squares positioning performance for agent 33 are shown in Fig. 5 with the corresponding sky-view and the building blockage area. The selected agent 33 is located in an environment surrounded by multiple buildings introducing severe reflection interferences, resulting in a poor GNSS least-squares positioning accuracy. By applying the Monte Carlo method with 10 samples, the collaborative positioning root-mean-square-error (RMSE) of agent 33 with other agents randomly selected based on the strategies of Open-sky CP, Mixed CP, and Dense urban CP are shown in Fig. 6 (a), (b), and (c), respectively.

The positioning performances from all three strategies outperform the conventional least-squares method, which validates the effectiveness of the 3DMA GNSS ray-tracing algorithm and the 3DMA GNSS based collaborative positioning algorithm. From the positioning performances of each Monte Carlo sample of different collaborated networks, the positioning strategy only involving collaborators in the open-sky environment (Open-sky CP) achieves a more robust performance compared to Mixed CP and Dense urban CP. On average, the Open-sky CP always outperforms the other two strategies on different network sizes. By involving more agents from the middle or dense urban environment, the collaborative positioning performance will be degraded. For the collaborative positioning, the larger network size has better potential to reduce the noise [4]. The Open-sky CP obtains a better error reduction slope with respect to the network size compared to other strategies. Noted the network size N=1 denotes the case in which the target agent does not collaborate with others, and only employs the absolute constraint and inter-epoch dynamic constraint to apply optimization. For the collaboration only with dense urban agents, many of the ray-tracing-corrected relative position constraints are still severely degraded or even unavailable. Hence, as Fig. 6 (c) shows, the collaboration with other agents under Dense urban CP is ineffective, even by involving more agents. For the best performance among all samples, Open-sky CP has a similar performance with Middle urban CP, whereas the Dense urban CP is still much worse than others.

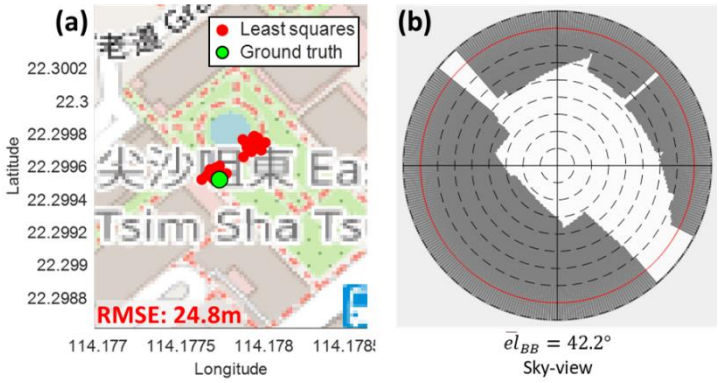

Fig. 5 (a) Ground truth and GNSS least-squares performance of agent 33; (b) Sky-view of agent 33 location, where the grey area denotes the sky-view being blocked by the buildings.

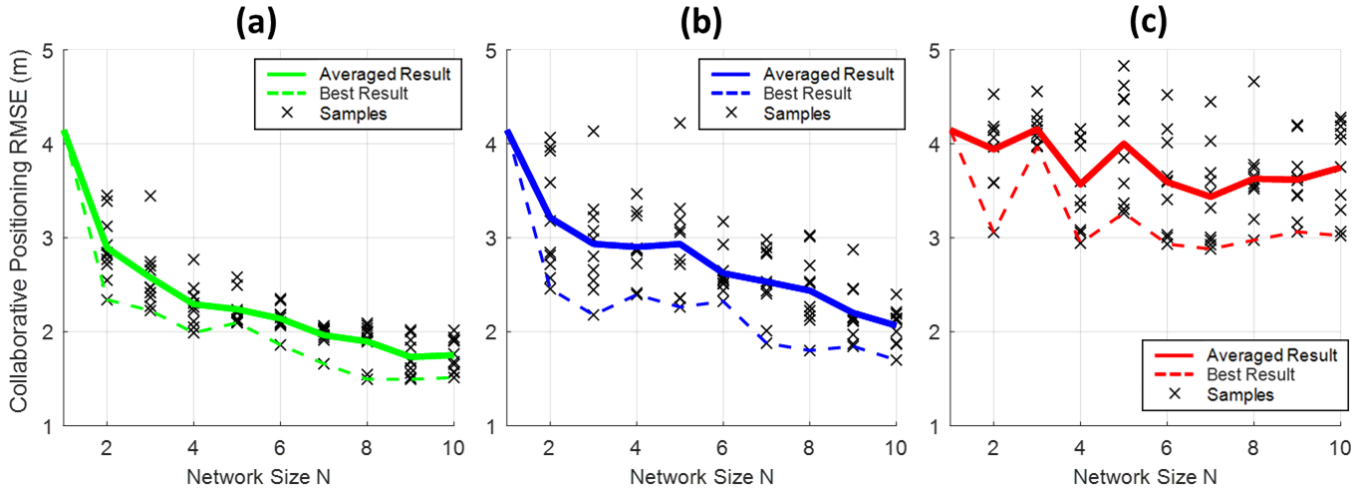

Fig. 6 Collaborative positioning performance of agent 33 with other agents selected by the strategy: (a) Open-sky CP; (b) Mixed CP; and (c) Dense urban CP. Black crosses denote Monte Carlo method samples.

Then, another agent located in a dense urban environment (agent 36) is selected to apply the same analysis on different agent selection strategies. The environment information and the collaborative positioning performance with different strategies for agent 36 are shown in Fig. 7. The GNSS measurements of this agent are significantly degraded by the reflection interferences due to the nearby buildings, which has an averaged elevation angle of 48.8°. The positioning error still remains 18 meters after applying optimization with the absolute position constraints from 3DMA GNSS ray-tracing positioning and the inter-epoch dynamic constraints from Doppler measurements. By applying the 3DMA GNSS collaborative positioning with relative position constraints, the positioning RMSE can be greatly reduced. Among different strategies, the Open-sky CP achieves the best performance in terms of accuracy and robustness, whereas the Dense urban CP is the worst. The positioning performances from different strategies for all agents are demonstrated in Appendix Fig. A, which shows that the Open-sky CP achieves the best performance for most cases.

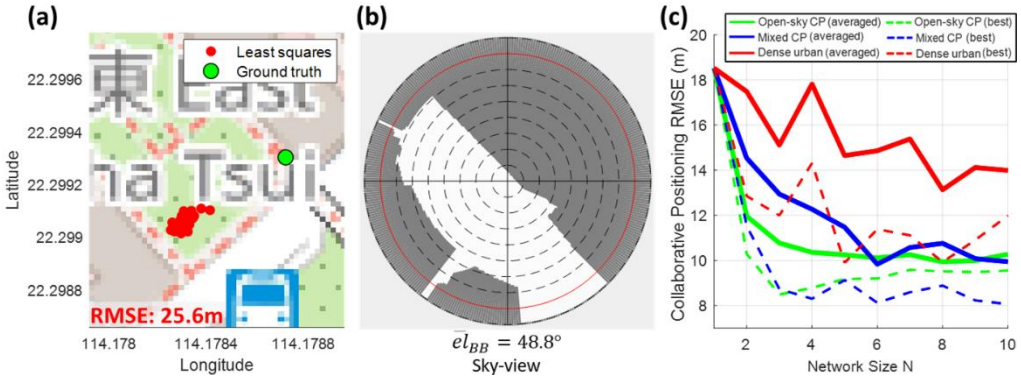

Fig. 7 (a) Ground truth and GNSS least-squares solutions of agent 36; (b) Sky-view with building blockages for agent 36; (c) Collaborative positioning performance of agent 36 with other agents selected by different strategies.

The benefits of Open-sky CP are probably because it has a higher potential to guarantee the qualities of the absolute position constraints (Eq. 5) during the collaborative positioning. The averaged absolute positioning constraint error of each agent during collaborative positioning is shown in Fig. 8 for the East and North directions. The averaged relative positioning constraint errors on the East and North direction between different agents during collaborative positioning are shown by the color in Fig. 9. For the open-sky agent (No. 1 - 15), the corresponding absolute position constraints are much better than those of other agents from the middle or dense urban. On the other hand, the relative position constraints involving open-sky agents will not be worse than the constraint between urban agents. Therefore, those open-sky agents can be regarded as accurate anchors during the collaborative positioning for a target agent degraded in urban areas. However, for some agents (e.g., agent 41), the relative positioning constraint error is always large, no matter which agent it is collaborating with or in which environment. This is probably due to the remained error from the target after ray-tracing correction, which is still unique and unable to be canceled by collaborative positioning. As a result, the performance of collaborative positioning under Open-sky CP could still be limited by the qualities of relative positioning constraints. In summary, selecting the agent from an open-sky environment for collaborative positioning guarantees the quality of absolute position constraint, which can obtain a better performance compared to the collaboration without agent selection. The performance of collaborative positioning could still be limited by the quality of relative position constraint, even by collaborating with open-sky agents.

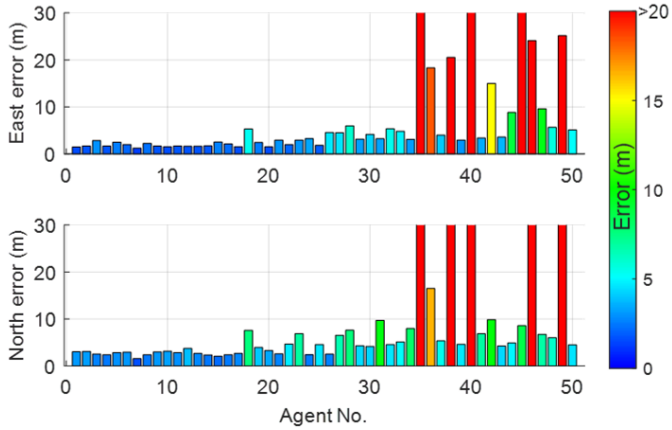

Fig. 8 Averaged (over all epochs) absolute positioning constraint error for each agent during collaborative positioning. The color denotes the error level. The y-axes are scaled with an upper limit of 30 meters.

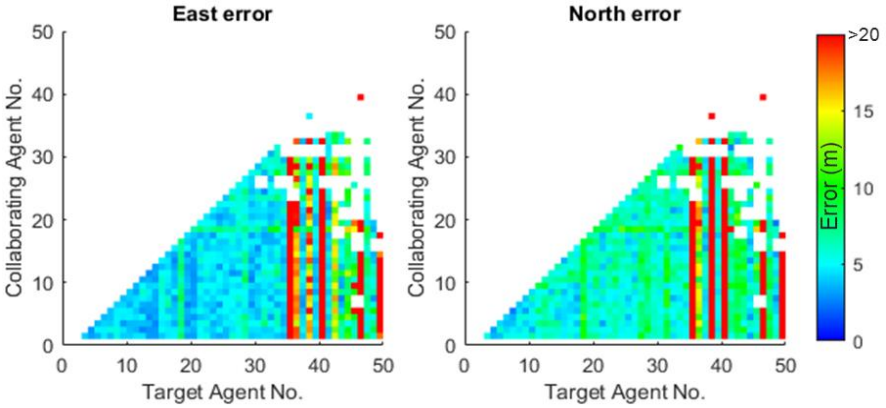

Fig. 9 Averaged (over all epochs) relative positioning constraint error between different agents during collaborative positioning. The color denotes the error level. The constraint between a pair of agents and its inverse pair is the same and is only shown once.

5. PERFORMANCE ANALYSIS ON SPATIALLY CORRELATED AGENTS

From the analysis result of agent 33 (Fig. 6), we notice that some samples involving urban agents may achieve a better collaborative position performance than the network only involving open-sky agents. By selecting a special case as seen in Fig. 10, the collaboration between agent 33 and 32, we find both agents are located in a similar environment with three sides surrounded by buildings (the sky-views in Fig. 6 and Fig. 10). Their GNSS measurement error could be similar or correlated due to the similar environmental geometrical parameters. Hence, some unique errors may become spatially correlated and can be canceled during the collaborative positioning, resulting in a better performance than collaborating with open-sky agents. To further investigate the occurrence of spatial correlation and its benefits, we conduct an analysis on the collaborative positioning of multiple agents purposely distributed in an area with similar environments.

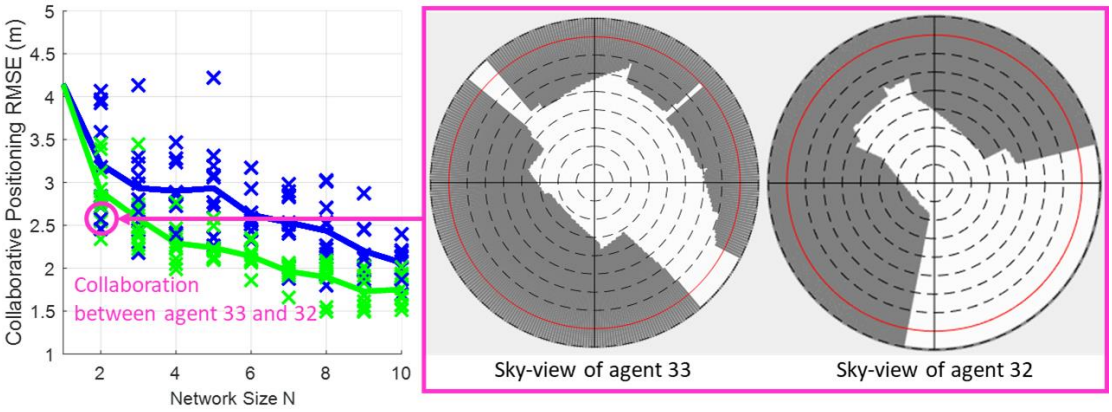

Fig. 10 A special case of collaboration (between agent 33 and 32) with urban agents achieving better performance.

5.1. Simulation Scenario Setup

For the GNSS reflected signal, the introduced delay is closely related to the orientation of the reflected surface and the distance between the agent and the reflected surface [28]. Agents with the same distance to buildings along the same street have a higher potential to encounter spatial correlation on the GNSS pseudorange error. Therefore, we set up a simulation extending Section 4.1 with nine agents evenly distributed with 5 meters in-between in along- or cross-street direction to analyze the spatial correlation on collaborative positioning, as Fig. 11 shows. These agents are assigned with the index from 51 to 59. The collaborative positioning performance is analyzed by the Monte Carlo method sampling different network combinations according to two strategies:

(1) Open-sky CP: Select collaborator from open-sky agents ($\overline{el}_{BB}$ below 15°, agents 1-15 in Section 4);
(2) Correlated CP: Select collaborator from the agents along the same street (among agents 51-59);

After comparing the positioning performance between Open-sky CP and Correlated CP, we select a representative case to analyze the behavior of the GNSS measurement error spatial correlation and its benefit to the collaborative positioning.

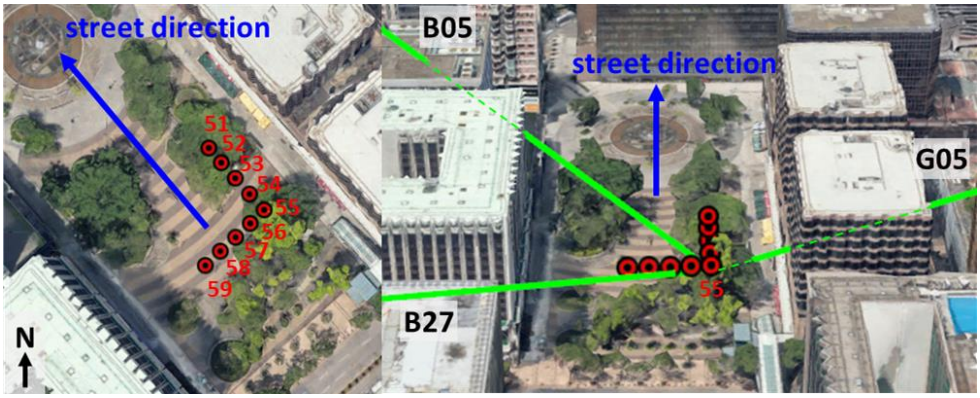

Fig. 11 Simulation setup for the analysis of GNSS measurement spatial correction on collaborative positioning.

5.2. Collaborative Positioning Performance and Measurement Behaviors of the Spatial Correlated Agents

Firstly, we select agent 55 in the center, having the highest potential to be spatially correlated with more agents, as the target agent to apply collaborative positioning with other agents according to two strategies, Open-sky CP and Correlated CP. The positioning performances by the Monte Carlo method corresponding to different network sizes are shown in Fig. 12. Since the agent combination is limited by the 8 collaborators in Correlated CP, the Monte Carlo method is applied with only 7 samples. The result shows that the Correlated CP achieves a performance similar or even better than the Open-sky CP, although all the collaborators are located in the urban area with degraded absolute position constraint quality. The benefit is probably due to the quality improvement on relative position constraints from spatially correlated measurements.

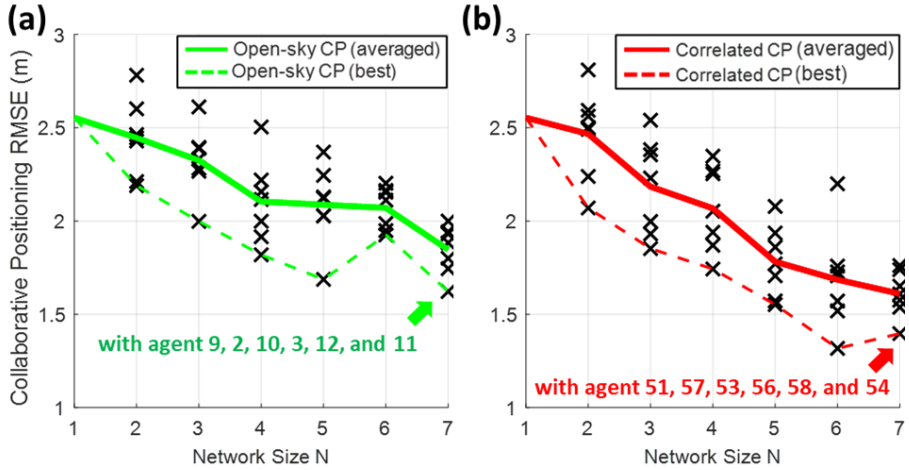

Fig. 12 The collaborative positioning performance of agent 55 as the target agent collaborating with other agents selected from the strategy (a) Open-sky CP; (b) Correlated CP. The best case in Open-sky CP is the collaboration with agents 9, 2, 10, 3, 12, and 11. The best case in Correlated CP is the collaboration with agents 51, 57, 53, 56, 58 and 54.

The pseudorange errors of three representative satellites for different agents from 51 to 59 are shown in Fig. 13. For satellite G05, the pseudorange measurements of agent 51-55 contain a similar NLOS reception error. Here, agents 51-55 are lined up along the street with the same distance to the building. However, the NLOS reception error of agent 56, adjacent to agent 55 in the cross-street direction, starts to deviate from other agents' errors. For agent 57-59 distributed on the cross-street direction, the pseudorange is affected by multipath rather than NLOS reception, resulting in a totally different error pattern. For the satellite B05, although all the pseudorange errors for different agents belong to the same type (NLOS reception), the error similarity is reduced when the agents are on different locations on the cross-street direction, especially for agents with longer distance in-between, e.g., agent 55 and agent 59. This is probably due to the difference in the distance between the agent and the reflecting surface of the building. For satellite B27 under multipath effects, the pseudorange errors are not similar even for the adjacent agents on the along-street direction. This is probably because the multipath error also depends on the phase difference between each signal, which is sensitive to the signal propagation geometry. In summary, the NLOS reception error on pseudorange has a good spatial correlation behavior for agents on the along-street direction, but such spatial correlation is reduced on the cross-street direction, especially for agents with a longer distance in-between. However, the multipath errors are less likely to be spatially correlated on the along-/cross-street direction due to the dependency on the phase difference between signals.

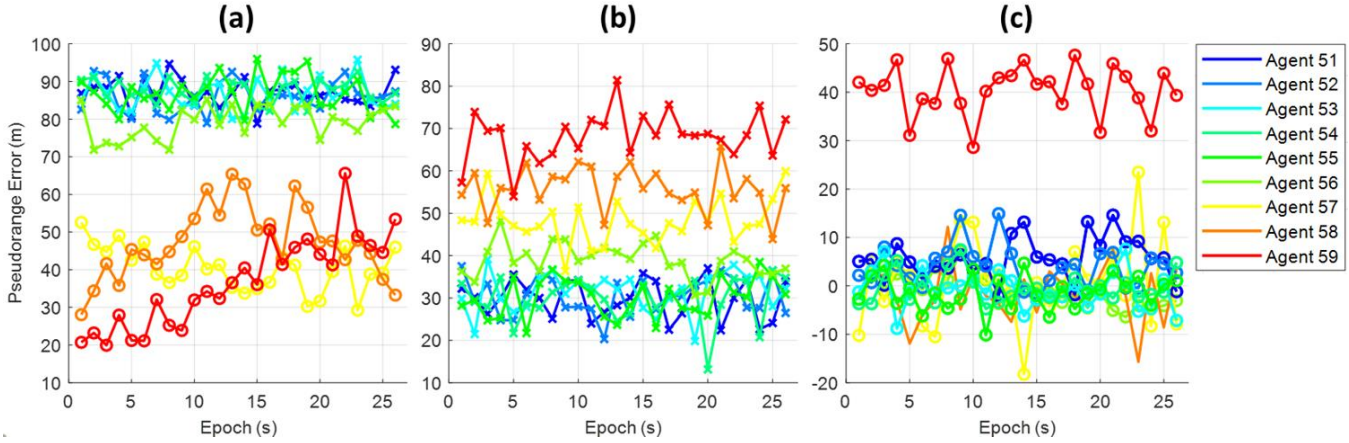

Fig. 13 The pseudorange errors from different agents for the satellite (a) G05; (b) B05; and (c) B27. The marker denotes the error type, where "x", "o", and "none" are NLOS reception, multipath, and LOS, respectively.

Two sets of collaboration networks obtaining the best performance on Open-sky CP and Correlated CP are selected to analyze the benefits of GNSS measurement spatial correlation on the collaborative positioning. The RMSEs of the relative position constraints between different agents for the agent selection strategy of Open-sky CP and Correlated CP are demonstrated in Tables 1 and 2, respectively. On average, agents with spatial correlation achieve better qualities on relative position constraints than open-sky agents, even though the measurements are severely degraded. Due to the spatial correlation on pseudorange error, those NLOS reception errors from different agents become correlated and similar, which can be directly mitigated by applying the DD method. Then, the accuracy of the DD estimated relative position (Eq. 3) as well as the $\Delta\hat{\boldsymbol{x}}_{k_a k_b}$ and $\Delta\tilde{\boldsymbol{x}}_{k_a k_b}$ matching process for relative position constraint estimation (Eq. 4) could be improved. As a result, a higher quality of the relative position constraint (Eq. 6) could be achieved for the spatial correlated agents.

Table 1 The RMSEs (m) of the relative position constraint between different agents during the best collaborative positioning case in Open-sky CP

Index		Collaborating agent						
		55	9	2	10	3	12	11
Target agent	55		7.0	8.0	8.2	7.8	6.7	7.7
	9			9.5	10.4	6.9	12.8	10.8
	2				6.5	8.6	7.7	8.2
	10					7.7	9.2	9.1
	3						10.9	9.9
	12							9.8
	11	Average: 8.7						

Table 2 The RMSEs (m) of the relative position constraint between different agents during the best collaborative positioning case in Correlated CP

Index		Collaborating agent						
		55	51	57	53	56	58	54
Target agent	55		8.3	8.9	7.0	8.3	8.3	6.2
	51			10.2	8.5	7.5	5.9	7.3
	57				9.5	10.0	12.5	9.4
	53					8.3	6.5	6.4
	56						8.4	8.5
	58							7.9
	54	Average: 8.3						

However, during collaborative positioning, the performance may not be solely determined by the relative position constraint between one pair of agents on all epochs. For example, the relative position constraint between agents *a* and *b* might be the best for the first epoch, but worse than between agents *a* and *c* for the second epoch. It is necessary to find the best relative position constraint epoch-wise to evaluate the overall collaborative positioning performance of a network. Therefore, we use the concept of optimal constraint link to conduct the evaluation. For the target agent *a* inside the collaboration network with *N* agents at epoch *t*, the optimal constraint link $b_t^* \rightarrow a$ and its accumulated error $\sigma_{ocl,t}$ are obtained by

$$b_t^* = \underset{b\in\{1,\cdots,N\}}{arg\ min}\left(\left|\sigma_{b,t}\right| + \left|\sigma_{ab,t}\right|\right) \tag{12}$$

$$\sigma_{ocl,t} = \left|\sigma_{b_t^*,t}\right| + \left|\sigma_{ab_t^*,t}\right| \tag{13}$$

where $\sigma_{b,t}$ is the error of absolute position constraint for agent *b*, $\sigma_{ab,t}$ is the error of relative position constraint between agent *a* and *b*. The optimal constraint link can be used to describe the best combination of constraints to estimate the target agent position at a specific epoch. The optimal constraint link errors $\sigma_{ocl,t}$ during the collaborative positioning of the strategy Open-sky CP and Correlated CP are demonstrated in Fig. 14 on the East and North directions. The RMSEs of $\sigma_{ocl,t}$ for different strategies are summarized in Table 3. For many of the epochs, the Correlated CP has a lower optimal constraint link error compared to the Open-sky CP, which has a higher potential to achieve better positioning accuracy for the target agent according to the available constraints. The Correlated CP also achieves lower RMSEs for the optimal constraint link errors than Open-sky CP, which obtains higher potential to achieve better collaborative positioning performance (as Fig. 12 shows). In summary, the agents with spatial correlation can obtain relative position constraints with better qualities, which enhance the capability on position estimation and further improve the performance of collaborative positioning, even better than the collaboration with agents in an open-sky environment.

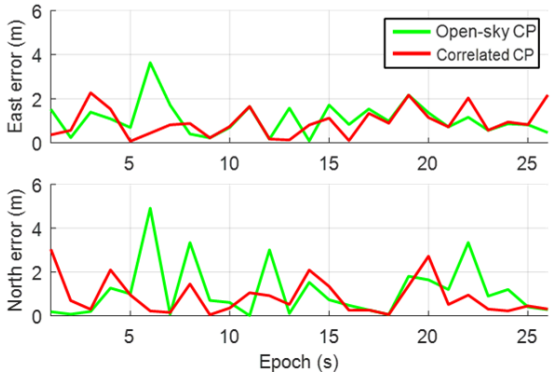

Fig. 14 The optimal constraint link error ($\sigma_{ocl,t}$) on each epoch for the collaborative positioning with the strategy of Open-sky CP or Correlated CP.

Table 3 The RMSE (m) of the optimal constraint link on all epochs during the collaborative positioning with different agent selection strategies.

Direction	East	North
Open-sky CP	**1.3**	**1.7**
Correlated CP	**1.2**	**1.2**

6. CONCLUSION AND FUTURE WORKS

In this study, we firstly analyze the influence from the environment of agents for the GNSS collaborative positioning. Based on a realistic urban GNSS simulator (GNSS RUMS) and a 3DMA GNSS based collaborative positioning algorithm, the collaborative positioning performance is evaluated through Monte Carlo simulation with three environment-based agent selection strategies, collaborate with open-sky agents only, all agents, or dense urban agents only. The analysis result shows that collaborating with open-sky agents can guarantee the qualities of the absolute position constraints employed in the optimization process, achieving a better collaborative positioning performance than without an agent selection. However, some of the samples involving collaborators from similar urban environments may obtain performances comparing to the collaboration with only open-sky agents. Then, we analyze the collaborative positioning with the agents lined up along/cross the same street, which are expected to have similar signal reflection geometry. The analysis shows that the NLOS reception errors are spatially correlated for agents along the street with the same distance to the building. Such correlation reduces by the distance between agents in the cross-street direction. The spatial correlation on the multipath error may not be observed due to the phase difference between each signal. The spatially correlated agents can achieve better relative position constraints by using the DD method to mitigate those similar NLOS reception errors. As a result, the capability of a spatially correlated network on obtaining accurate positioning estimation will be enhanced, which is even comparable to the collaboration with open-sky agents only.

However, we only conduct a qualitative analysis of the spatial correlation on GNSS measurements. A quantitative analysis on this spatial correlation needs to be conducted in the future, in order to develop an indicator to evaluate the correlation level and the benefits to the collaborative positioning. Besides, the noise covariance determines the weighting of each constraint during the optimization process. The accuracy of the noise covariance estimation will significantly affect the effectiveness of an accurate constraint, either an absolute position constraint from an open-sky agent or a relative position constraint between spatially correlated agents. Therefore, the estimation of a proper noise covariance matrix for each constraint during the collaborative positioning will be another future work.

APPENDIX

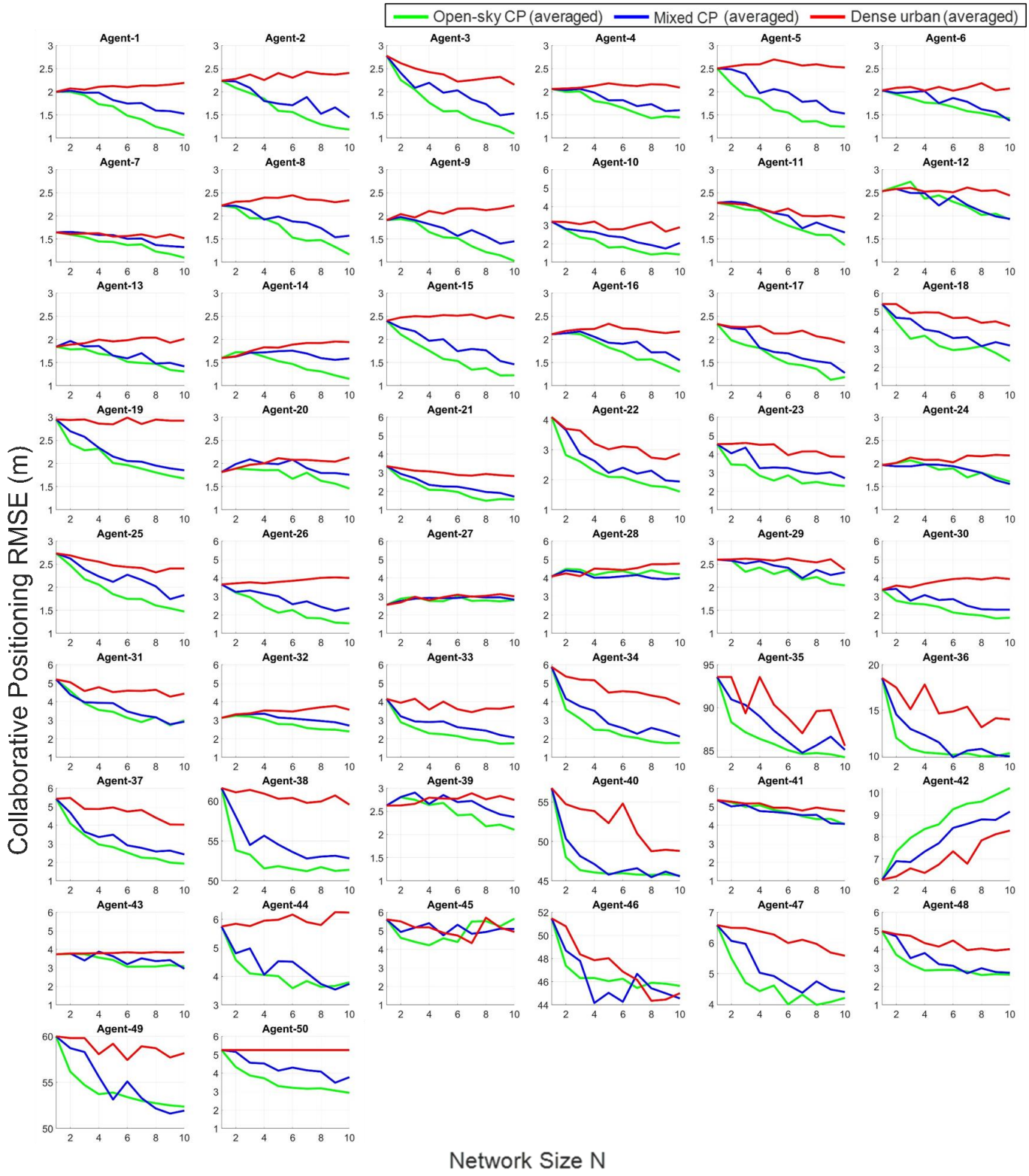

Fig. A Collaborative positioning performance of each agent as the target to apply different agent selection strategies.

REFERENCE

1. de Ponte Müller, F., *Survey on ranging sensors and cooperative techniques for relative positioning of vehicles.* Sensors, 2017. **17**(2): p. 271.

2. Alam, N., A.T. Balaei, and A.G. Dempster, *Relative positioning enhancement in VANETs: A tight integration approach.* IEEE Transactions on Intelligent Transportation Systems, 2013. **14**(1): p. 47-55.
3. Liu, K., et al., *Improving positioning accuracy using GPS pseudorange measurements for cooperative vehicular localization.* IEEE Transactions on Vehicular Technology, 2014. **63**(6): p. 2544-2556.
4. Pirani, M., et al., *Cooperative Vehicle Speed Fault Diagnosis and Correction.* IEEE Transactions on Intelligent Transportation Systems, 2018(99): p. 1-7.
5. Minetto, A., A. Nardin, and F. Dovis. *Tight Integration of GNSS Measurements and GNSS-based Collaborative Virtual Ranging*. in *Proceedings of the 31st International Technical Meeting of the Satellite Division of The Institute of Navigation (ION GNSS+ 2018)*. 2018. Miami, Florida.
6. Bhamidipati, S. and G.X. Gao, *GPS Multireceiver Joint Direct Time Estimation and Spoofer Localization.* IEEE Transactions on Aerospace and Electronic Systems, 2019. **55**(4): p. 1907-1919.
7. Groves, P., *Multipath vs. NLOS signals.* Inside GNSS, 2013. **8**(6): p. 40-42.
8. Bisnath, S.B. and R.B. Langley. *Pseudorange multipath mitigation by means of multipath monitoring and de-weighting*. in *Proceedings of KIS*. 2001.
9. Tmazirte, N.A., et al. *Sigma-Z: A New Parametric and Constrained-by-Design GNSS Observation Weighting Model for Land Applications*. in *Proceedings of the 2021 International Technical Meeting of The Institute of Navigation*. 2021.
10. Walter, T. and P. Enge. *Weighted RAIM for precision approach*. in *Proceedings of the 8th International Technical Meeting of the Satellite Division of The Institute of Navigation (ION GPS 1995)*. 1995. Palm Springs, CA: Institute of Navigation.
11. Hsu, L.-T., et al., *Multiple Faulty GNSS Measurement Exclusion Based on Consistency Check in Urban Canyons.* IEEE Sensors Journal, 2017. **17**(6): p. 1909-1917.
12. Zhang, G., W. Wen, and L.-T. Hsu. *A novel GNSS based V2V cooperative localization to exclude multipath effect using consistency checks*. in *Position, Location and Navigation Symposium (PLANS), 2018 IEEE/ION*. 2018. Monterey, CA: IEEE.
13. Wang, L., P.D. Groves, and M.K. Ziebart, *Smartphone shadow matching for better cross-street GNSS positioning in urban environments.* The Journal of Navigation, 2015. **68**(3): p. 411-433.
14. Zhang, G., W. Wen, and L.-T. Hsu, *Rectification of GNSS-based collaborative positioning using 3D building models in urban areas.* GPS Solutions, 2019. **23**(3): p. 83.
15. Tanwar, S. and G.X. Gao. *Multi-Epoch Multi-Agent Collaborative Localization Using Grid-based 3DMA GNSS and Inter-Agent Ranging*. in *Proceedings of the 32nd International Technical Meeting of the Satellite Division of The Institute of Navigation (ION GNSS+ 2019)*. 2019. Miami, Florida.
16. Hsu, L.-T., Y. Gu, and S. Kamijo, *3D building model-based pedestrian positioning method using GPS/GLONASS/QZSS and its reliability calculation.* GPS Solutions, 2016. **20**(3): p. 413-428.
17. Zhang, G., et al., *3D Mapping Database Aided GNSS Based Collaborative Positioning Using Factor Graph Optimization.* IEEE Transactions on Intelligent Transportation Systems, 2020: p. 1-13.
18. Zhang, G., et al. *Scalability and Latency Analysis of the Centralized 3D Mapping Aided GNSS-Based Collaborative Positioning*. in *Proceedings of the 2021 International Technical Meeting of The Institute of Navigation*. 2021.
19. Icking, L., T. Kersten, and S. Schön. *Evaluating the Urban Trench Model For Improved GNSS Positioning in Urban Areas*. in *2020 IEEE/ION Position, Location and Navigation Symposium (PLANS)*. 2020.
20. Zhang, G., et al., *GNSS RUMS: GNSS Realistic Urban Multiagent Simulator for Collaborative Positioning Research.* Remote Sensing, 2021. **13**(4): p. 544.
21. Liu, X., S. Nath, and R. Govindan. *Gnome: A Practical Approach to NLOS Mitigation for GPS Positioning in Smartphones*. in *Proceedings of the 16th Annual International Conference on Mobile Systems, Applications, and Services*. 2018. ACM.
22. Dellaert, F., *Factor graphs and GTSAM: A hands-on introduction*. 2012, Georgia Institute of Technology.
23. Kouyoumjian, R.G. and P.H. Pathak, *A uniform geometrical theory of diffraction for an edge in a perfectly conducting surface.* Proceedings of the IEEE, 1974. **62**(11): p. 1448-1461.
24. Zavorotny, V.U. and A.G. Voronovich, *Scattering of GPS signals from the ocean with wind remote sensing application.* IEEE Transactions on Geoscience and Remote Sensing, 2000. **38**(2): p. 951-964.
25. Liu, L. and M.G. Amin, *Tracking performance and average error analysis of GPS discriminators in multipath.* Signal Process., 2009. **89**(6): p. 1224–1239.
26. Xie, P. and M.G. Petovello, *Measuring GNSS Multipath Distributions in Urban Canyon Environments.* IEEE Transactions on Instrumentation and Measurement, 2015. **64**(2): p. 366-377.
27. Wen, W., et al. *UrbanLoco: A Full Sensor Suite Dataset for Mapping and Localization in Urban Scenes*. in *2020 IEEE International Conference on Robotics and Automation (ICRA)*. 2020.
28. Hsu, L.-T., *Analysis and modeling GPS NLOS effect in highly urbanized area.* GPS solutions, 2018. **22**(1): p. 7.